

CODIMENSION 2 SYMMETRIC HOMOCLINIC BIFURCATIONS AND APPLICATION TO 1:2 RESONANCE

CHENGZHI LI AND CHRISTIANE ROUSSEAU

1. Introduction. In this paper we study a codimension 3 form of the 1:2 resonance. It was first noted by Arnold [3] that the study of bifurcations of symmetric vector fields under a rotation of order q yields information about Hopf bifurcation for a fixed point of a planar diffeomorphism F with eigenvalues $e^{2\pi ip/q}$. The map F^q can be identified to arbitrarily high order with the flow map of a symmetric vector field having a double-zero eigenvalue ([3], [4], [10], [23]). The resonance of order 2 (also called 1:2 resonance) considered here is the case of a pair of eigenvalues -1 with a Jordan block of order 2. The diffeomorphism then has normal form around the origin given by [4]:

$$(1.1) \quad F(x, y) = (-x + y + O(|x, y|^n), -y + a_1x^3 + b_1x^2y + a_2x^5 + b_2x^4y + \dots + O(|x, y|^n)).$$

In the non-degenerate case of codimension 2, we have $a_1, b_1 \neq 0$. We study the codimension 3 case $a_1 \neq 0, b_1 = 0, b_2 \neq 0$, for which we have the unfolding:

$$(1.2) \quad F_\mu(x, y) = (-x + y + O(|x, y|^n), \mu_1x + (\mu_2 - 1)y + a_1x^3 + \mu_3x^2y + b_2x^4y + \dots + O(|x, y|^n)).$$

The square of this map F_μ^2 is, up to higher-order terms, the flow map of a symmetric system:

$$(1.3) \quad \begin{aligned} \dot{x} &= y \\ \dot{y} &= \epsilon_1x + \epsilon_2y + ax^3 + \epsilon_3x^2y + bx^4y + cx^5 + O(|x, y|^6) \quad a, b \neq 0. \end{aligned}$$

The purpose of this paper is to give the bifurcation diagram of (1.3) and to prove that (1.3) is a universal unfolding of the same system at $\epsilon = 0$. The techniques are quite standard:

Determination of the phase portrait of (1.3):

- study of singular points and Hopf bifurcations,
- transformation of the system into a near-Hamiltonian system, and determination of the limit cycles and homoclinic loops as zeros of elliptic integrals;

Received March 23, 1988 and in revised form September 1, 1989. This work was supported by NSERC and by the Québec Ministry of Education.

Proof that (1.3) is a universal unfolding: this uses techniques similar to those developed in [11] for the cusp of order 3.

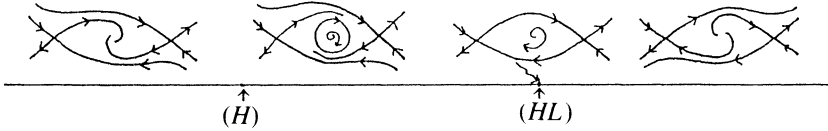


Figure 1. Birth of a limit cycle through a Hopf bifurcation and death in a heteroclinic connection.

Codimension 2 homoclinic bifurcations appear in system (1.3). Depending on the sign of a , these are of two kinds. For $a > 0$ we have a heteroclinic loop through two symmetric saddle points, and for $a < 0$ a pair of symmetric homoclinic loops through the origin (we call this, a *symmetric homoclinic loop*, and the corresponding bifurcation, a *symmetric homoclinic loop bifurcation*). In both cases, because of the symmetry of the vector fields, a neighborhood of the homoclinic (resp. heteroclinic) connection is studied by a Poincaré map which has the same asymptotic expansion as for a single homoclinic loop ([11], [21]). There is a major qualitative distinction between symmetric homoclinic and heteroclinic loop bifurcations. The latter leads to the emergence or disappearance of limit cycles (Figure 1) as for the usual homoclinic loop bifurcation. In the former, limit cycles “pass through” the loop, in the same way as zeros of a function change sign (Figure 2).

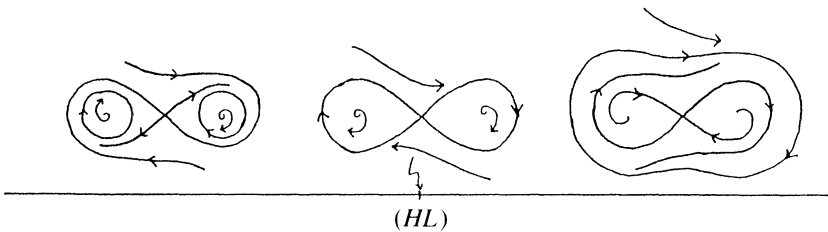


Figure 2. A symmetric homoclinic loop bifurcation of order 1.

Our analysis is very similar to the analysis of the cusp of order 3 for the 1:1 resonance. When $a > 0$ it is exactly the same, and we call this a *symmetric cusp of order 3* (partly because of its similarity to the case of order 3, partly because of the topological shape of the vector field before unfolding). The cusp of order n has been extensively studied in the literature ([5] and [6] for $n = 2$, [11] for $n = 3$, [17] for $n = 4$, [15], [19], [22] for the general case). All results transpose exactly for the symmetric cusp of order n : the bifurcation diagram is the same, and we can also conclude that there is a maximum number of $(n - 1)$ limit cycles. In the case $a < 0$ an analysis of higher codimensions remains to be done.

In Section 2 we discuss the normal form of a symmetric system with a double-zero eigenvalue. In Section 3, we derive the bifurcation diagram of (1.3). In Section 4 we discuss the universality of (1.3). We conclude with several remarks on the application to 1:2 resonance.

Notation. For all bifurcation curves (or surfaces) in all figures:

- (H) denotes Hopf bifurcation, (H_2) , Hopf bifurcation of order 2, etc ...
- (HL) denotes the double homoclinic (or heteroclinic) loop bifurcation, (HL_2) the same bifurcation of codimension 2, etc ...
- $(2C)$ (resp. $(3C)$) denotes double (resp. triple) limit cycle bifurcation.
- $(2C_{\text{ext}})$ (resp. $(2C_{\text{int}})$) denotes double external (resp. internal) limit cycle bifurcation, in the case $\eta = -1$.
- (P) denotes pitchfork bifurcation.
- (DZ) denotes double-zero eigenvalue bifurcation.

2. Normal form of a symmetric system with a double-zero eigenvalue.

We consider a symmetric system around the origin, with linear part given by:

$$(2.1) \quad \begin{aligned} \dot{x} &= y \\ \dot{y} &= 0. \end{aligned}$$

Its normal form, first given by Takens [26], is:

$$(2.2) \quad \begin{aligned} \dot{x} &= y \\ \dot{y} &= a_1x^3 + a_2x^5 + \dots + b_1x^2y + b_2x^4y + o(|x, y|^6). \end{aligned}$$

We consider a system for with $a_1 \neq 0$. Under the change of coordinates (inspired from [22])

$$(2.3) \quad a_1X^4/4 = a_1x^4/4 + a_2x^6 + a_3x^8/8 + \dots,$$

and division by a symmetric positive function, system (2.2) becomes

$$(2.4) \quad \begin{aligned} \dot{X} &= y \\ \dot{y} &= a_1X^3 + c_1X^2y + c_2X^4y + yo(|X, y|^5). \end{aligned}$$

When $c_1 \neq 0$ the singularity at the origin has codimension 2. For the codimension 3 case, we have $c_1 = 0, c_2 \neq 0$. Rescaling $c_2 = -1, a_1 = \pm 1 = \eta$, we start with a normal form (setting $X = x$)

$$(2.5) \quad \begin{aligned} \dot{x} &= y \\ \dot{y} &= \eta x^3 - x^4y + yo(|x, y|^5), \end{aligned}$$

for which we study the unfolding

$$(2.6) \quad \begin{aligned} \dot{x} &= y \\ \dot{y} &= \epsilon_1x + \epsilon_2y + \epsilon_3x^2y + \eta x^3 - x^4y + yo(|x, y|^5), \end{aligned}$$

For a codimension n singularity with $a_1 \neq 0$, we would study the following unfolding:

$$(2.7) \quad \begin{aligned} \dot{x} &= y \\ \dot{y} &= \epsilon_1 x + \epsilon_2 y + \epsilon_3 x^2 y + \cdots + \epsilon_n x^{2(n-2)} y + \eta x^3 - x^{2(n-1)} y + y o(|x, y|^{2n-1}). \end{aligned}$$

The normal form is simpler here than for the cusp of order n , since all terms $x^{2m}y$ have independent contributions.

3. Bifurcation diagram of system (2.6). The singular points of (2.6) are given by $(0, 0)$ and $q_{\pm} = (\pm(-\eta\epsilon_1)^{1/2}, 0)$, when $\eta\epsilon_1 < 0$. The origin is a node or focus (resp. saddle) for $\epsilon_1 < 0$ (resp. $\epsilon_1 > 0$). The points q_{\pm} are nodes or foci (resp. saddles) for $\epsilon_1 > 0$ (resp. $\epsilon_1 < 0$). At $\epsilon_1 = 0$ we have a pitchfork bifurcation.

The system (2.6) has a Hopf bifurcation at the origin for $\epsilon_2 = 0, \epsilon_1 < 0$. Hopf bifurcation is of order 1 (resp. 2) on $\epsilon_3 \neq 0$ (resp. $\epsilon_3 = 0$). We have one attractive (resp. 2, one repulsive inside one attractive) limit cycle(s) inside the region $\epsilon_2 > 0$ ($\epsilon_2 < 0, \epsilon_3 > 0$).

The points q_{\pm} undergo a Hopf bifurcation (only in the case $\eta = -1$) on

$$\epsilon_2 + \epsilon_3 \epsilon_1 - \epsilon_1^2 + o(\epsilon_1^2) = 0.$$

Hopf bifurcation is of order 2 if $\epsilon_3 = 0$. The second Lyapunov coefficient is positive, and we have one (resp. two) limit cycles(s) in the region

$$\epsilon_2 + \epsilon_3 \epsilon_1 - \epsilon_1^2 + o(\epsilon_1^2) < 0,$$

(resp. $\epsilon_2 + \epsilon_3 \epsilon_1 - \epsilon_1^2 + o(\epsilon_1^2) > 0, \epsilon_3 > 0$) (cf. [17] for a brief explanation of the method of Lyapunov coefficients and [24] for a detailed one).

For $\epsilon_1 = \epsilon_2 = 0$, the origin has a codimension 2 bifurcation with a nilpotent linear part. This bifurcation has been studied in the literature ([7], [13], [14], [25]). The bifurcation diagrams for $\eta = \pm 1$ are given in Figure 3.

To follow the growth of the limit cycles around the origin if $\eta = 1$, and around q_{\pm} if $\eta = -1$, we make the change of coordinates

$$(3.1) \quad \begin{aligned} x &= \delta u & \epsilon_1 &= -\eta \delta^2 \mu_0 \\ y &= \delta^2 v & \epsilon_2 &= \delta^4 \mu_1 \\ \tau &= \delta t & \epsilon_3 &= \delta^2 \mu_2, \end{aligned}$$

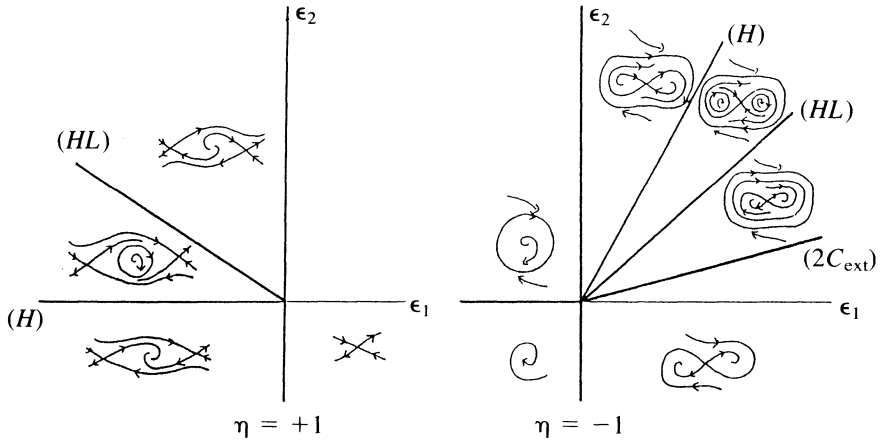


Figure 3. Bifurcation diagram of the codimension 2 system with nilpotent linear part.

and we get the system:

$$(3.2) \quad \begin{aligned} u' &= v \\ v' &= -\eta\mu_0u + \eta u^3 + \delta^3(\lambda_1v + \mu_2u^2v - u^4v) + o(\delta^4), \end{aligned}$$

which we study as a perturbation of the Hamiltonian system:

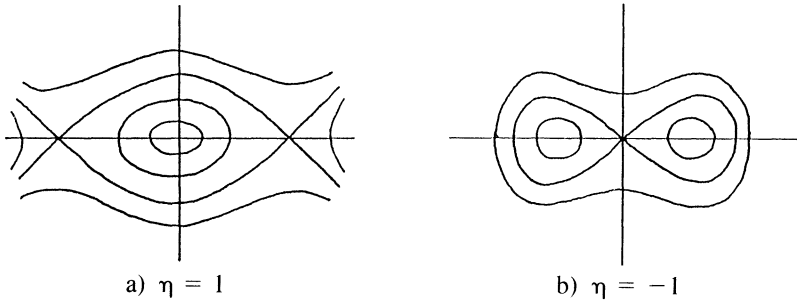


Figure 4. The Hamiltonian systems (3.3).

$$(3.3) \quad \begin{aligned} u' &= v \\ v' &= -\eta\mu_0u + \eta u^3, \end{aligned}$$

with Hamiltonian function (Figure 4):

$$(3.4) \quad H = v^2/2 + \eta\mu_0u^2/2 - \eta u^4/4.$$

The system has the form:

$$(3.5) \quad \begin{aligned} \dot{x} &= \partial H / \partial y + \epsilon f(x, y) + o(\epsilon) \\ \dot{y} &= -\partial H / \partial x + \epsilon g(x, y) + o(\epsilon). \end{aligned}$$

For small ϵ , we consider the ‘‘Poincaré return map’’ P on a section Σ , transversal to closed level curves of H (including possibly homoclinic or heteroclinic loops), and parametrized by values of H . As for the homoclinic loop bifurcation, depending on the position of the separatrices, it may happen that the return map going forward does not exist, and that one must consider the return map going backwards. Details for the special case appearing here will be given in Proposition 3.6. It is known that

$$(3.6) \quad P(h) - h = \epsilon \int_{H=h} g dx - f dy + o(\epsilon).$$

In order for a limit cycle (homoclinic or heteroclinic loop) to merge from a closed level curve $H = h$ (homoclinic or heteroclinic loop) at $\epsilon = 0$, it is necessary that

$$(3.7) \quad M(h) = \int_{H=h} g dx - f dy = 0.$$

For sufficiency, we need some non-degeneracy condition, for example $M'(h) \neq 0$, in which case we can apply the implicit function theorem to obtain a unique limit cycle for small ϵ . With a more degenerate condition as $M(h) = M'(h) = 0, M''(h) \neq 0$, a double limit cycle follows from the Malgrange–Weierstrass preparation theorem [16] or [20]. Similar conditions exist for a homoclinic loop [21].

Study of the zeros of M . In our system M is the function:

$$(3.8) \quad M(h) = \int_{H=h} (\mu_1 v + \mu_2 u^2 v - u^4 v) du.$$

This function is a linear combination of the $I_i(h)$, where

$$(3.9) \quad I_i(h) = \int_{H=h} u^{2i} v du.$$

As for the cusp of order n , we can remark that all I_i are linear combinations of I_0 and I_1 , the coefficients of which are polynomials in h . This goes through the induction formula given in the following proposition:

PROPOSITION 3.1.

$$(3.10) \quad (2n + 3)I_n = 4n\mu_0 I_{n-1} - 4h\eta(2n - 3)I_{n-2}, \quad \text{for } n \geq 2.$$

In particular:

$$(3.11) \quad I_2 = -4h\eta I_0/7 + 8\mu_0 I_1/7.$$

Proof. This derivation is quite standard (see for example [11] or [22]). It is understood here that all integrals are taken on the curve $H = h$.

$$\begin{aligned} (3.12) \quad I_n &= \int u^{2n} v du = \int (u^{2n} - \mu_0 u^{2n-2}) v du + \mu_0 I_{n-1} \\ &= \int \eta u^{2n-3} v^2 dv + \mu_0 I_{n-1} \\ &= -\eta(2n-3)/3 \int v^3 u^{2n-4} du + \mu_0 I_{n-1} \\ &= -\eta(2n-3)/3 \int v u^{2n-4} (-\eta\mu_0 u^2 + 2h + \eta u^4/2) du + \mu_0 I_{n-1} \\ &= -(2n-3)I_n/6 + 2n\mu_0 I_{n-1}/3 - 2h\eta(2n-3)I_{n-2}/3. \end{aligned}$$

PROPOSITION 3.2. i) I_0 and I_1 satisfy the Picard-Fuchs equations:

$$(3.13) \quad \begin{aligned} I_0 &= 4hI'_0/3 - \eta\mu_0 I'_1/3, \\ I_1 &= 4h\mu_0 I'_0/15 + (-4\eta\mu_0^2 + 12h)I'_1/15. \end{aligned}$$

ii) If we define $P = I_1/I_0$, then P satisfies a Riccati equation:

$$(3.14) \quad 4h(4h - \eta\mu_0^2)P' = -5\eta\mu_0 P^2 + 8hP + 4\eta\mu_0^2 P - 4\mu_0 h.$$

Proof. The proof can be found in [10]. It is similar to the derivation of a Riccati equation in the case of a cusp [11].

We will consider $P(h)$ as trajectory of the vector field:

$$(3.15) \quad \begin{aligned} \dot{h} &= -4h(\mu_0^2 - 4\eta h) \\ \dot{P} &= -5\mu_0 P^2 + 8\eta h P - 4\eta\mu_0 h + 4\mu_0^2 P. \end{aligned}$$

The vector field is sketched in Figure 5 for the case $\eta = -1$. (The case $\eta = 1$ is obtained through $h \mapsto -h$.)

The curve $H = h$ contains:

i) for $\eta = 1$ and $\mu_0 > 0$: a closed component around the origin for $h \in (0, 1/4)$. The values $h = 0$ and $h = 1/4$ correspond to the origin and the heteroclinic loop.

ii) for $\eta = -1$ and $\mu_0 > 0$:

– two closed components, one around each of the points $(\pm 1, 0)$ for $h \in (-1/4, 0)$. The value $h = -1/4$ corresponds to the two points $(\pm 1, 0)$, while $h = 0$ corresponds to symmetric homoclinic loop.

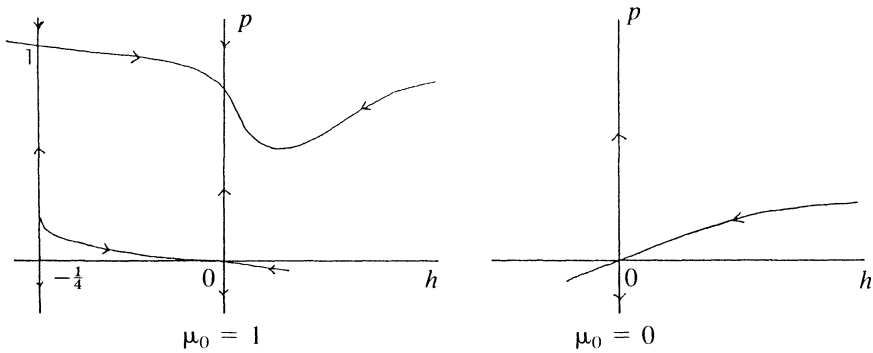


Figure 5. Phase portrait of the system (3.15).

– a closed component surrounding the three singular points for $h > 0$.

iii) for $\eta = -1$ and $\mu_0 \leq 0$: a closed component around the origin for $h > 0$.

PROPOSITION 3.3. For $\eta = -1$ and $\mu_0 = 1$:

i) The graph of $P(h)$ for $h \in [-1/4, 0]$, is the unstable separatrix of saddle point $(-1/4, 1)$. It joins $(-1/4, 1)$ to the node $(0, 4/5)$.

$$(3.16) \quad \text{ii) } P(-1/4) = 1, \quad P(0) = 4/5.$$

$$(3.17) \quad \text{iii) } P([-1/4, 0] \subset [4/5, 1].$$

$$(3.18) \quad \text{iv) } P' < 0 \text{ for } h \in [-1/4, 0], P'(-1/4) = -1/2, P'(0) = -\infty.$$

$$(3.19) \quad \text{v) } P(h) > 1/2 \text{ for } h > 0.$$

vi) $P'(h)$ has a unique zero for $h = h^* > 0$, is negative for $h < h^*$ and positive for $h > h^*$.

vii) $P(h) \rightarrow +\infty$ when $h \rightarrow +\infty$.

$$(3.20) \quad \text{viii) } P''(h) < 0 \text{ for } h \in [-1/4, 0].$$

$$(3.21) \quad \text{ix) } P''(h) > 0 \text{ for } h > 0 \text{ and } P'(h) \leq 0.$$

$$(3.22) \quad \text{x) } P(h) \sim kh^{1/2} \text{ with } k > 0, \text{ for } h \rightarrow +\infty.$$

xi) There exists a unique $\tilde{h} > h^*$ such that

$$(3.23) \quad P''(\tilde{h}) = 0, \quad P''(h) > 0 \text{ for } 0 < h < \tilde{h}, \quad P''(h) < 0 \text{ for } h > \tilde{h}.$$

Proof. The proofs for all these properties are essentially the same as for the similar function P in the case of a cusp [11]. We detail the cases which are not similar.

$$\text{v) } \dot{P}|_{P=1/2} = 3/4 > 0.$$

vi) and vii) See proof in [7].

viii) We can check that $P''(-1/4) < 0$. Suppose now that $P''(\hat{h}) = 0$ and $P''(h) < 0$ for $h < \hat{h} < 0$. Since:

$$(3.24) \quad 2h(1 + 4h)P'' = P'(5P - 12h - 4) + (4P - 2),$$

$$(3.25) \quad 2h(1 + 4h)P''' = P'(5P' - 8) + P''(5P - 28h - 6),$$

then, at point \hat{h} , (3.25) gives $P'''(\hat{h}) < 0$, which is a contradiction.

ix) This follows from (3.24).

x) The argument here is similar to the argument in [7].

$$(3.26) \quad I_i = 4 \int_0^c u^{2i} \sqrt{u^2 - \frac{u^4}{2} + 2h} \, du,$$

where c is the unique positive root of $u^2 - u^4/2 + 2h = 0$, for h sufficiently large. When $h \rightarrow +\infty$, $c \sim h^{1/4}$. We let $u = cz$ in (3.26):

$$(3.27) \quad I_i = c^{2i+3} \int_0^1 z^{2i} \sqrt{\frac{1-z^4}{2} + \frac{z^2-1}{c^2}} \, dz \sim c^{2i+3} \int_0^1 z^{2i} \sqrt{\frac{1-z^4}{2}} \, dz,$$

for h sufficiently large. Accordingly, $P = I_1/I_0 \sim kc^2 \sim kh^{1/2}$, with

$$(3.28) \quad k = \frac{\int_0^1 z^2 \sqrt{1-z^4} \, dz}{\int_0^1 \sqrt{1-z^4} \, dz} \approx 0.274.$$

xi) From ix) and x) there exists a positive h such that $P''(h) = 0$. Let \tilde{h} be the first such h . Necessarily $P'''(\tilde{h}) \leq 0$. So, by (3.25), $P'(\tilde{h}) \leq 8/5$. We consider first the case $P'''(\tilde{h}) < 0$. Suppose now that $P''(h_1) = 0$, with $h_1 > \tilde{h}$. $P'(h_1) < P'(\tilde{h}) < 8/5$. From (3.19) and (3.24) we know that zeros of $P'(h)$ occur with $P''(h) > 0$. Therefore $P'(h_1) > 0$. This gives $P'''(h_1) < 0$, which is a contradiction. In the case $P'''(\tilde{h}) = 0$, we have $P'(\tilde{h}) = 8/5$. From this we get

$$P^{(4)}(\tilde{h}) = \dots = P^{(n)}(\tilde{h}) = \dots = 0.$$

This is in contradiction to the fact that P is analytic but non-polynomial in the neighborhood of \tilde{h} . (P is not polynomial since $P'(0) = -\infty$.)

These properties are summarized in Figure 5. The case $\eta = 1$ is obtained through a change of coordinates $h \mapsto -h, P \mapsto 1 - P$ (since $P(0) = 1/5, P(1/4) = 0$).

PROPOSITION 3.4. For $\eta = -1$ and $\mu_0 = 0, P = k\sqrt{h}$ for $h > 0$, where k is given in (3.28).

Proof. This follows from (3.14) and an argument as in Proposition 3.3 when $h \rightarrow +\infty$.

PROPOSITION 3.5. For $\eta = -1$ and $\mu_0 < 0$:

i) The graph of $P(h)$ for $h > 0$ is the stable separatrix of the saddle point $(0, 0)$.

$$(3.29) \quad \text{ii) } P' < 0 \text{ for } h > 0.$$

$$(3.30) \quad \text{iii) } P'' < 0 \text{ for } h > 0.$$

$$(3.31) \quad \text{iv) } P(h) \sim Kh^{1/2} \text{ with } K > 0, \text{ for } h \rightarrow +\infty$$

with k given in (3.28).

Proof. This is the same as for Proposition 3.3.

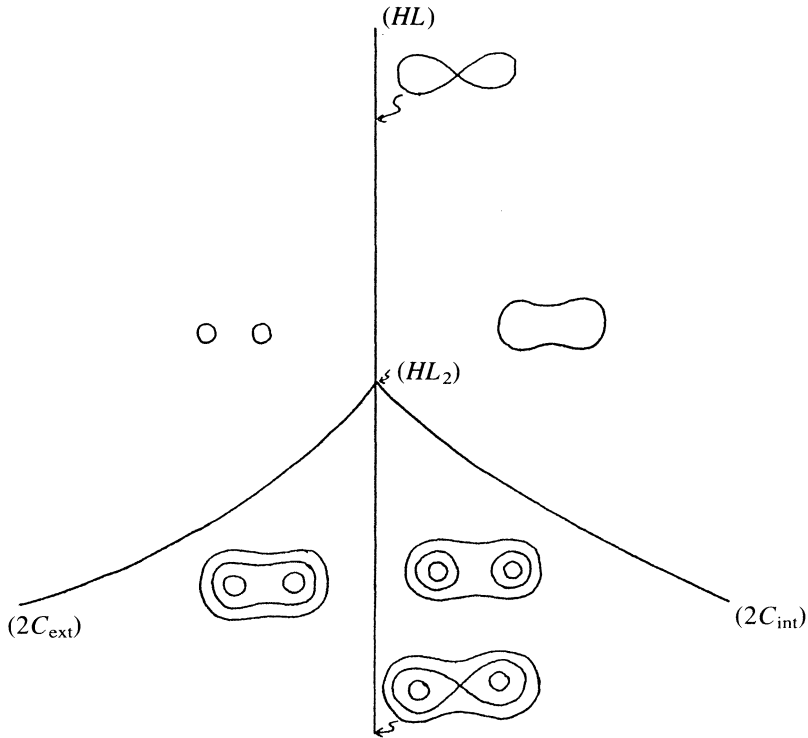


Figure 6. The symmetric homoclinic loop bifurcation diagram of order 2. We have represented only the limit cycles and not the separatrices.

PROPOSITION 3.6. The bifurcation diagram for the symmetric homoclinic loop bifurcation of order 2 is given in Figure 6.

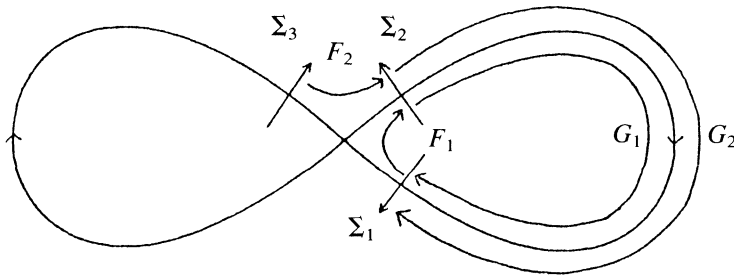


Figure 7. Return map in the neighborhood of the double homoclinic loop.

Proof. We consider a “return map” in the neighborhood of the symmetric homoclinic loop. For this we consider sections $\Sigma_1, \Sigma_2, \Sigma_3$ as in Figure 7. Parametrization on the Σ_i is given by h , which is zero on the loop and increasing in the direction of the arrows. The return map inside one of the loops is given by $H_1 = G_1 \circ F_1$. When the loops are destroyed, the map H_1 is not always defined. The map $H_1^{-1} = F_1^{-1} \circ G_1^{-1}$ is then defined. In both cases looking for limit cycles is the same as looking for points h such that $F_1(h) = G_1^{-1}(h)$. Similarly, outside the symmetric homoclinic loop, half of the return map is given by $H_2 = G_2 \circ F_2$. We have $G_2(h) = G_1(-h)$ and $F_2(h) = F_1(-h)$. Because of the symmetry the return map outside the double loop is given by H_2^2 . Since H_2 is monotonic, H_2^2 has a fixed point if and only if H_2 has a fixed point. So we can speak of a “Poincaré map” given by H_1 for $h \leq 0$ and H_2 for $h > 0$. This map has exactly the same form as in the case of a simple homoclinic loop [21]. A fixed point of the map with $h > 0$ (resp. $h < 0$) corresponds to a large limit cycle around the three singular points (resp. a pair of small limit cycles). Around $h = 0$, $\bar{M}(h)$ has the asymptotic expansion:

$$(3.32) \quad \bar{M}(h) = c_0 + c_1 h \ln|h| + c_2 h + o(h).$$

The symmetric homoclinic loop bifurcation of order 2 occurs for $c_0 = c_1 = 0$. We then have $c_2 < 0$. For $c_0 < 0, c_1 < 0$ (resp. $c_1 > 0$) we always have a negative (resp. positive) zero ($\ln|h| < 0$ for small $|h|$). In that region two positive (resp. negative) zeros occur for $|c_0| \ll |c_1| \ll |c_2|$, and disappear when $|c_0|$ and $|c_1|$ grow.

THEOREM 3.7. *The bifurcation diagram of the system (3.2) with δ sufficiently small and $\mu_0 = 1$ is given by Figure 8 (resp. Figure 9) in the case $\eta = -1$ (resp. $\eta = 1$).*

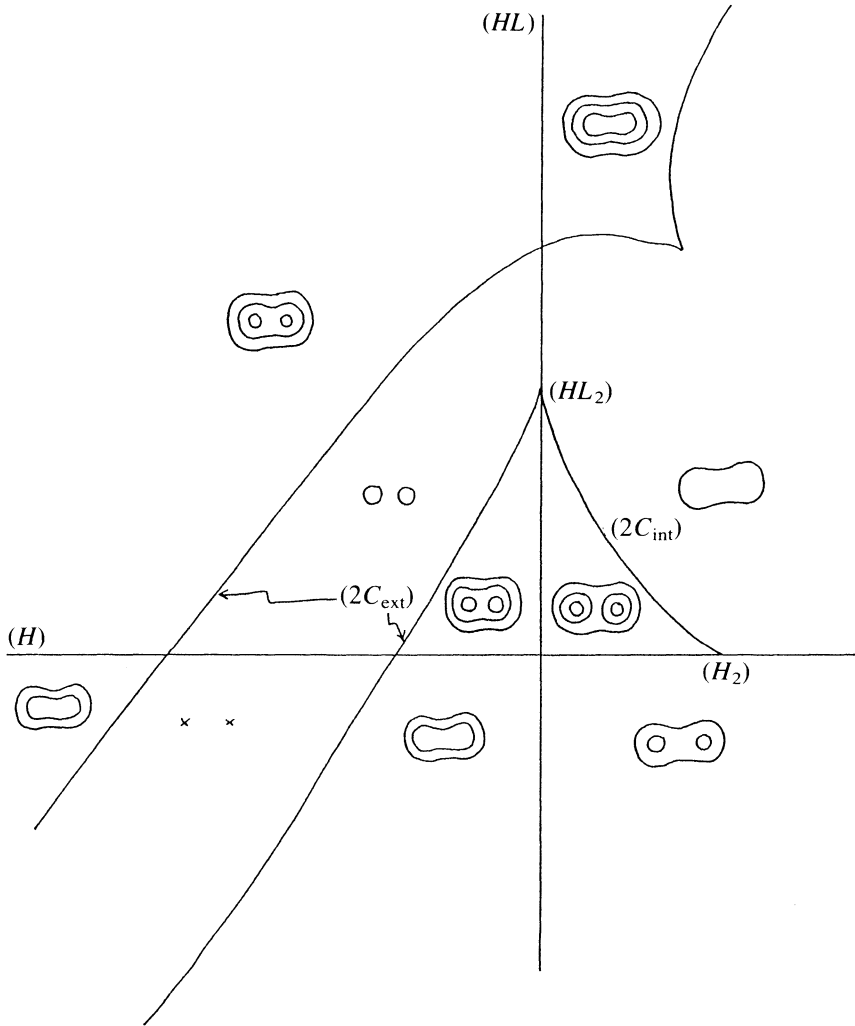


Figure 8. Bifurcation diagram of (3.2) in the μ -plane ($\mu_0 = 1, \eta = -1$). The picture is only qualitative.

Proof. This follows from the bifurcation diagram of the zeros of $M(h)$. We give details for the case $\eta = -1$. The case $\eta = 1$ is simpler.

1) *Bifurcation diagram of the zeros of $M(h)$.* The function $M(h)$ in (3.8) is given by:

$$(3.33) \quad M(h) = (\mu_1 - 4h/7)I_0 + (\mu_2 - 8/7)I_1.$$

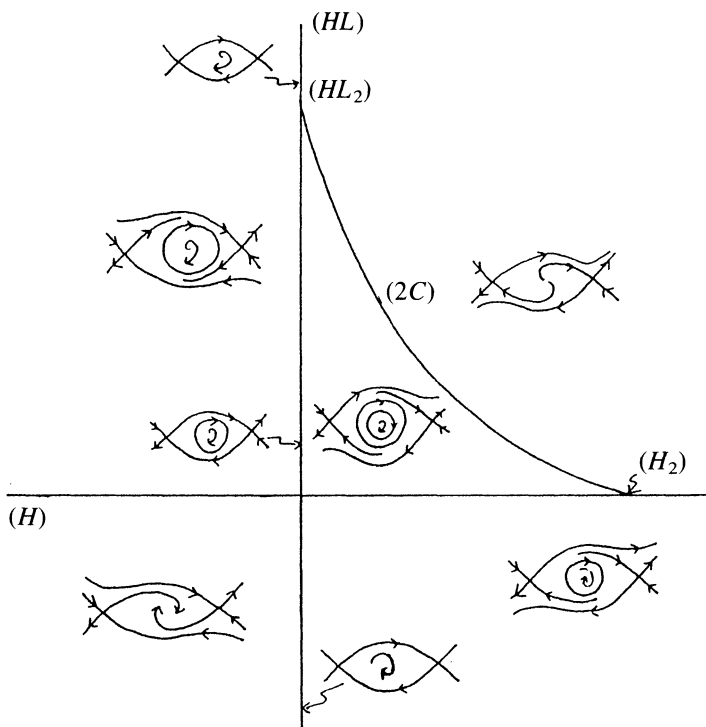


Figure 9. Bifurcation diagram of (3.2) in the μ -plane ($\mu_0 = 1, \eta = 1$). The picture is only qualitative.

Instead, we study the zeros of:

$$(3.34) \quad \bar{M}(h) = M(h)/I_0 = (\mu_1 - 4h/7) + (\mu_2 - 8/7)P.$$

Zeros of $\bar{M}(h)$ will be interpreted by intersection points of $P(h)$ with the line $\bar{M}(h) = 0$. From this geometric interpretation and the concavity (convexity) of the function $P(h)$ on $[-1/4, 0]$ (in the region $h > 0, P' < 0$), it follows directly, using Figure 5, that (see Figure 10 and at the same time the bifurcation diagram in the (μ_1, μ_2) variables in Figure 8):

- i) There is a maximum number of two (resp. three) internal (resp. external) limit cycles, i.e., that contain only one of the points $(\pm 1, 0)$ (resp. the three singular points) (Figure 10a and 10b).
- ii) In the case of two internal limit cycles, we necessarily have an external limit cycle at the same time (Figure 10a).
- iii) In the case of two external limit cycles, we have either one internal limit cycle or none at all (Figure 10c and 10d).

In the case of three external limit cycles, we have no internal limit cycle (Figure 10b).

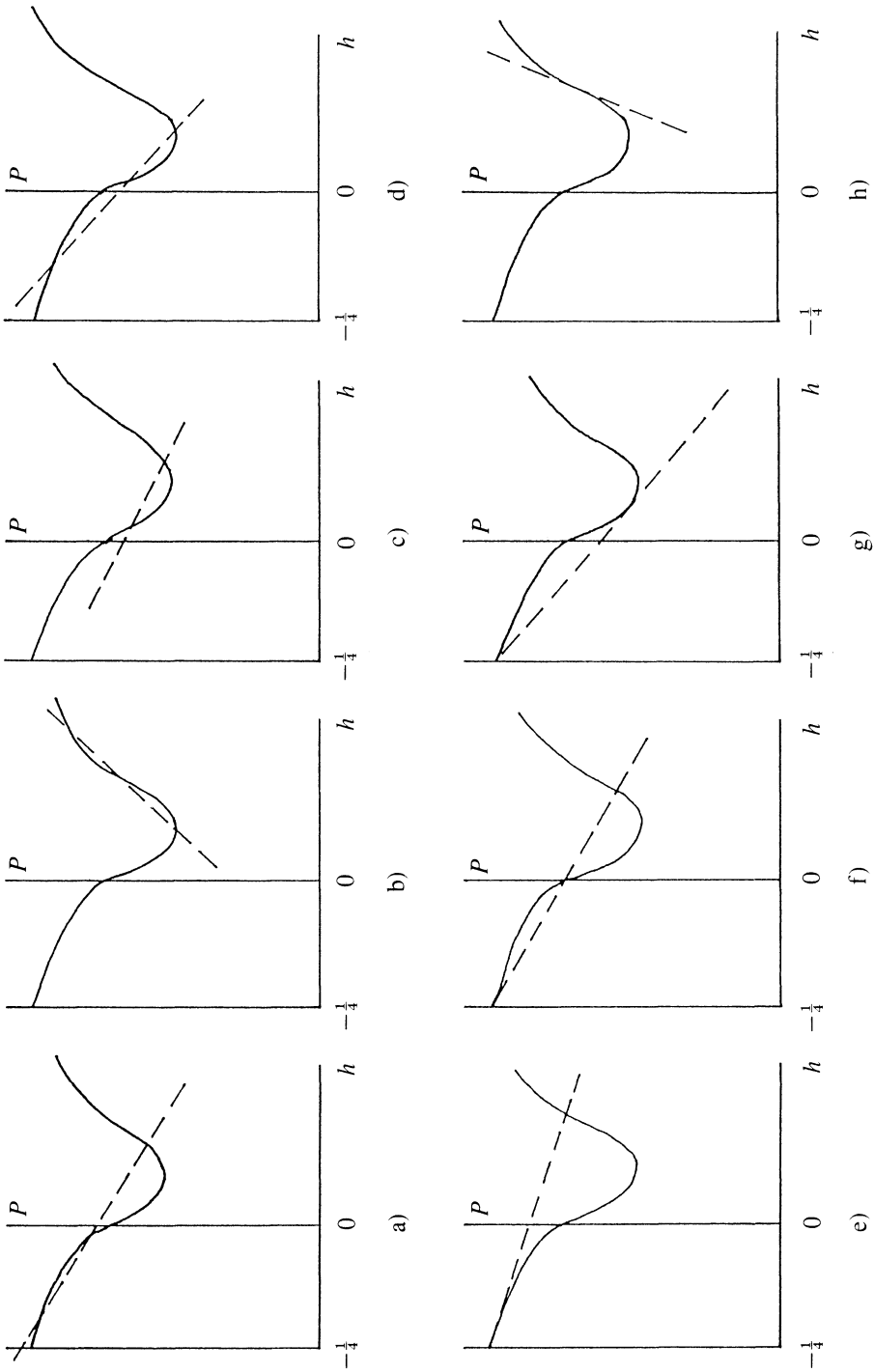


Figure 10. Some respective positions of $P(h)$ and $M(h) = 0$, giving different positions of limit cycles.

iv) Hopf bifurcation (resp. symmetric homoclinic loop bifurcation) of order 2 is given by a line tangent to $P(h)$ at the point $(-1/4, 1)$ (resp. $(0, 4/5)$). In the former (latter) the line has slope $-1/2$ (is vertical), which gives $\mu_2 = 0$ (Figure 10e) (resp. $\mu_2 = 8/7$).

v) Similarly a point of Hopf bifurcation simultaneous to a symmetric homoclinic loop bifurcation is given by a line $\tilde{M}(h) = 0$ passing through the points $(-1/4, 1)$ and $(0, 4/5)$, i.e., with slope $-4/5$. This yields $\mu_2 = 3/7$ (Figure 10f). There is a limit cycle surrounding the symmetric homoclinic loop.

vi) We have a point in the bifurcation diagram with a double external limit cycle, together with a Hopf bifurcation (Figure 10g).

vii) The curve of double internal limit cycles is a convex curve joining Hopf bifurcation of order 2 to symmetric homoclinic loop bifurcation of order 2. In fact, the lines $\tilde{M}(h) = 0$ have the form $\mu_2 = \mu_1 Q + R$, with $Q = -1/P$, and $R = 4/7(2 + h/P)$. It is easy to check that $-R$ is a convex function of Q . The curve of double internal limit cycles is the Legendre transform of $-R$. It is therefore the convex envelope of the lines $\tilde{M}(h) = 0$ (see the argument in [11]).

viii) The curve of double external limit cycles starts at the double homoclinic bifurcation of order 2 and crosses the Hopf bifurcation line (see iv). Between these two points the curve is convex, since $P''(h) > 0$ in that region (see Proposition 3.3 above).

viii) There is a point with a triple limit cycle (Figure 10h).

ix) When the slope of the line $\tilde{M}(h) = 0$ passes through zero from negative to positive, this corresponds to μ_2 going from $-\infty$ to $+\infty$.

In the case $\eta = 1$, the bifurcation is much simpler, and identical to the bifurcation diagram obtained in [11] (Figure 9).

2) *Bifurcation diagram of (3.2).* Limit cycles are given as zeros of

$$(3.35) \quad V(h) = \epsilon M(h) + o(\epsilon), \epsilon = \delta^3.$$

For $\epsilon \neq 0$ (our system has no limit cycle for $\epsilon = 0$), it is sufficient to consider zeros of $\tilde{V}(h) = V(h)/\epsilon$. If we have $M(h_0) = 0$ and $M'(h_0) \neq 0$, which gives

$$\tilde{V}(h_0)|_{\epsilon=0} = 0, \quad V'(h_0)|_{\epsilon=0} \neq 0$$

then, by implicit function theorem, we have a unique limit cycle for the system. Accordingly, simple zeros of $M(h)$ correspond to hyperbolic limit cycles. Similarly, if we have the conditions $M(h_0) = M'(h_0) = M^{(k-1)}(h_0) = 0$ and $M^{(k)}(h_0) \neq 0$, for $h_0 \in [-1/4, 0) \cup (0, +\infty)$, then by the Malgrange–Weierstrass preparation theorem [20]:

$$(3.36) \quad V(h) = Q(h - h_0, \epsilon)H(h, \epsilon)$$

in the neighborhood of h_0 , where Q is a monic polynomial in $(h - h_0)$ of degree k satisfying

$$Q(h - h_0, 0) = (h - h_0)^k,$$

and H is invertible around h_0 . We then have at most k limit cycles. Here we have the special cases $k = 2, 3$. When $k = 2, \bar{M}(h) = \bar{M}'(h) = 0, \bar{M}''(h) \neq 0$ gives

$$(3.37) \quad \begin{aligned} \mu_1 - 4h/7 + (\mu_2 - 8/7)P &= 0, \\ -4/7 + (\mu_2 - 8/7)P' &= 0, (\mu_2 - 8/7)P'' \neq 0. \end{aligned}$$

The second equation gives $h = h(\mu_2)$, and replacing in the first gives $\mu_1 = \mu_1(\mu_2)$. So the surface of double limit cycles satisfies $\epsilon_2 = \epsilon_2(\epsilon_1, \epsilon_3)$. Similarly, when $k = 3$, the curve of triple limit cycles has equation $\epsilon_3 = \epsilon_3(\epsilon_1)$, and $\epsilon_2 = \epsilon_2(\epsilon_1, \epsilon_3)$. The limit cycles are hyperbolic everywhere except on these curve and surface.

Around $h = 0$ we use the theory of Roussarie (see Proposition 3.6 and [21]).

4. Bifurcation diagram of (2.6).

4.1 Bifurcation diagram of (2.6) in the case $\eta = -1$.

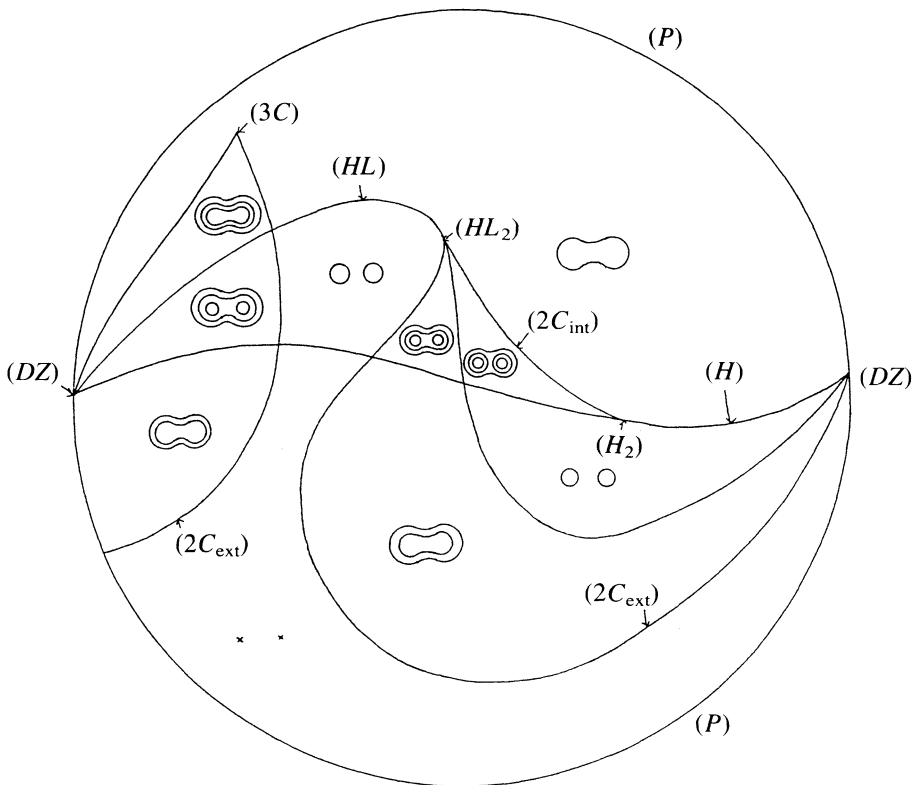


Figure 11. Intersection of the bifurcation diagram of (2.6) ($\eta = -1$) with a half-sphere around the origin, in the half-space $\epsilon_1 \geq 0$.

THEOREM 4.1. *The bifurcation diagram of (2.6) is given in Figure 11. The bifurcation diagram is a cone through the origin. Therefore a good way to represent it is to intersect it with a sphere around the origin. Since there is little interesting behaviour on the half sphere $\epsilon_1 \leq 0$, we show only what happens on the half-sphere $\epsilon_1 \geq 0$, which we identify with a closed ball, having boundary $\epsilon_1 = 0$ (Figure 11).*

Proof. The bifurcation diagram consists of:

- i) The plane $\epsilon_1 = 0$, which is the locus of pitchfork bifurcation.
- ii) A cone on the bifurcation diagram of (3.2) in the region $\epsilon_1 > 0$.
- iii) The Hopf bifurcation surface $\epsilon_2 = 0, \epsilon_1 < 0$ for the origin.
- iv) The line $\epsilon_2 = \epsilon_3 = 0, \epsilon_1 < 0$ of Hopf bifurcation of order 2.
- v) The double limit cycle surface in the half-space $\epsilon_1 < 0$.
- vi) The bifurcation diagram for the double-zero eigenvalue in the neighborhood of the line $\epsilon_1 = \epsilon_2 = 0, \epsilon_3 \neq 0$ (Figure 3). Branching from these bifurcation diagrams (one for $\epsilon_3 > 0$, one for $\epsilon_3 < 0$), are two Hopf bifurcation surfaces (one supercritical, one subcritical), two symmetric homoclinic loop bifurcation surfaces (one stable, one unstable), and two double external limit cycle surfaces (one stable, one unstable). These come from the bifurcation diagram of (3.2) (Figure 8), except for a double external limit cycle surface. The only possibility is that this surface originates from the double limit cycle surface of Hopf bifurcation of order 2 in the plane $\epsilon_1 < 0$. The point with a triple limit cycle in Figure 11 can be explained in the following way: near (DZ) the two smallest limit cycles coalesce on $(2C_{ext})$. The two largest limit cycles coalesce at the other end of the same $(2C_{ext})$ curve, since they arise from Hopf bifurcation in the region $\epsilon_1 < 0$.

The bifurcation diagram must be given in a full neighborhood of the origin which is constructed as a union of three cones following a technique in [22]:

- a cone C_1 constructed around the ϵ_1 -axis on an arbitrary compact in (μ_1, μ_2) -space;
- a cone C_2 around the ϵ_2 -axis constructed on an arbitrary compact in μ_2 -space, multiplied by a small neighborhood of 0 in μ_0 -space.
- a cone C_3 around the ϵ_3 -axis constructed on a small neighborhood of 0 in (μ_0, μ_1) -space.

For the cone C_1 , we note that the bifurcation diagram of (3.2) is only valid for (μ_1, μ_2) in a compact region. Therefore (using (3.1)) it gives the bifurcation diagram of (2.6) in a cone around the ϵ_1 -axis built on a compact domain. But the compact can be taken arbitrarily large. This gives the cone C_1 .

To construct the cones C_2 and C_3 we study the system in the plane $\epsilon_1 = 0$ (see Proposition 4.2 thereafter). In this plane we find structurally stable behaviour outside a neighborhood of the origin, except on $\epsilon_2 = 0$, and on the double limit cycle curve. In this neighborhood, the origin is a singular point of codimension 1 or 2, for which the unfolding is well known. The crucial step is introduced in [11]: following this example, we scale $\mu_1 = \pm 1$ to obtain C_2 . The system at $\mu_0 = 0$ has a unique limit cycle (resp. zero or two limit cycles, with a double

limit cycle between the two regions) for $\mu_1 = 1$ (resp. $\mu_1 = -1$) and μ_2 in an arbitrary compact. This remains so for μ_0 in a small neighborhood of zero. Using (3.1) we get a conic neighborhood of the ϵ_2 -axis.

Similarly, for the cone C_3 we scale $\mu_2 = \pm 2$. The system at $\mu_0 = \mu_1 = 0$ has a unique limit cycle (resp. no limit cycle) for $\mu_2 = 2$ (resp. $\mu_2 = -2$). This remains so for (μ_0, μ_1) in a small neighborhood of zero. By (3.1) we get C_3 .

The universality of the unfolding for pitchfork bifurcation ensures us that small perturbations do not create limit cycles around the singular points q_{\pm} .

It remains to show how to extend the results obtained by rescaling, i.e., only valid in a domain in (x, y) -space depending on δ to a fixed domain in (x, y) -space. The technique used here is exactly the same as in [12] (focus case), and we only give the main lines. We have to show that all limit cycles can be studied by means of the rescaling, i.e., the limit cycles shrink to zero when the parameters approach the origin as in (3.1). For this purpose we introduce the maps

$$(4.1) \quad \begin{aligned} \phi_\delta: \mathbf{R}^2 &\rightarrow \mathbf{R}^2, (x, y) \mapsto (\delta x, \delta^2 y), \\ \psi_\delta: \mathbf{R}^3 &\rightarrow \mathbf{R}^3, \epsilon = (\epsilon_1, \epsilon_2, \epsilon_3) \mapsto (\delta^2 \mu_0, \delta^4 \mu_1, \delta^2 \mu_2). \end{aligned}$$

For A (resp. K) compact neighborhood of $0 \in \mathbf{R}^3$ in parameter-space (resp. $0 \in \mathbf{R}^2$ in phase-space) we consider $A_\delta = \psi_\delta(A)$, and $K_\delta = \phi_\delta(K)$. We look for compact neighborhoods A° of $0 \in \mathbf{R}^3$ and K° of $0 \in \mathbf{R}^2$, such that for all $\delta \in (0, 1]$ and for all $\epsilon \in A_\delta^\circ$, the orbits of X_ϵ passing through points of ∂K° have for positive time a point in common with ∂K_δ° . K° will be limited by a level curve $H = h$ of the Hamiltonian function H in (3.4). The idea is the following. For sufficiently small A we have a return map defined on ∂K and sending m to $\tilde{m} = rm$ with $0 < r < 1$ (r depends on m). Instead of working with small δ we replace δ by δv , with $\delta \in (0, 1]$ and $0 < v < v_0$. The return map on $\partial K_{\delta v}$ is given by

$$(4.2) \quad 1/\delta v [H(\tilde{m}) - H(m)] = \int_{H=h} -u^4 v^2 dt + O(\mu_1) + O(\mu_2) + O(v).$$

If A and v_0 are sufficiently small, this quantity is negative. We choose $A^\circ = \phi_{v_0}(A)$ and $K^\circ = \psi_{v_0}(K)$. Let $\delta \in (0, 1]$, $\epsilon \in A_\delta^\circ$, and $m \in \partial K^\circ$. Then for any $\delta' \in [\delta, 1]$, the X_ϵ -orbit of $m_{\delta'} = \phi_{\delta'}(m)$ will cut $[0, m]$ in a point $m_{\delta''} = r_{\delta''} m_{\delta'}$ with $r_{\delta''} < 1$, i.e., $\delta'' < \delta'$. As $[\delta, 1]$ is compact, the X_ϵ -orbit of m will finally have to cut ∂K_δ° .

PROPOSITION 4.2. *For $\epsilon_1 = 0$, the bifurcation diagram consists of the line $\epsilon_2 = 0$. From it branches a double limit cycle curve. This completes the proof that the bifurcation diagram of (2.6) is given in Figure 12.*

Proof. We use equation (3.2) with $\mu_0 = 0$. As in Theorem 3.7 we first study the zeros of $\tilde{M}(h)$. The double-zero occurs at $\tilde{M}(h) = \tilde{M}'(h) = 0$, i.e.,

$$(4.3) \quad \mu_1 = -4h/7 \quad \mu_2 = 8\sqrt{h}/7k, \quad h > 0.$$

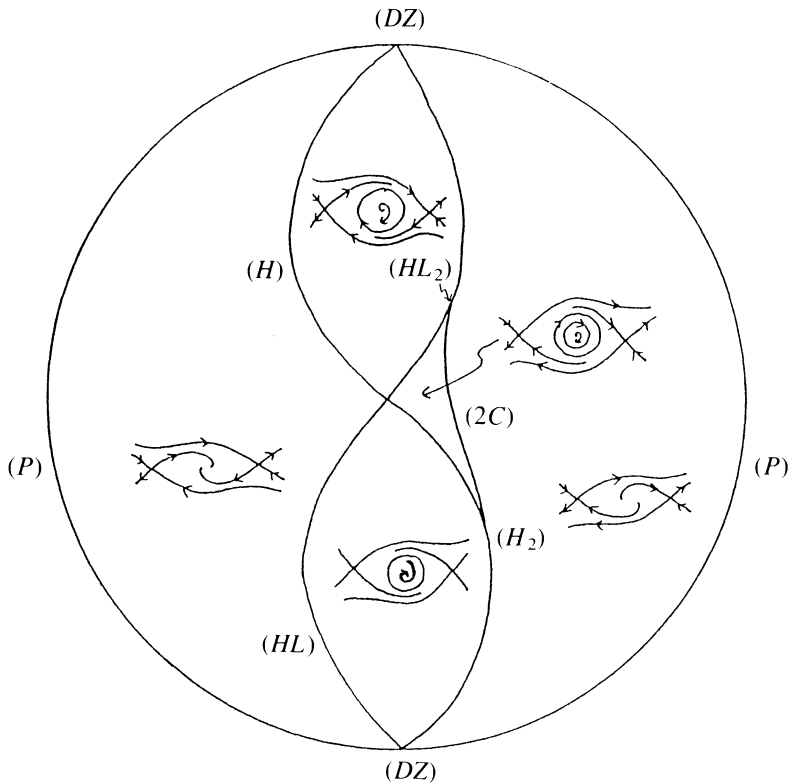


Figure 12. Intersection of the bifurcation diagram of (2.6) with a half-sphere in $\epsilon_1 \cong 0$ for $\eta = 1$.

This gives:

$$(4.4) \quad \mu_2^2/\mu_1 = -16/(7k^2), \quad \mu_2 > 0, \quad \mu_1 < 0,$$

where k is precisely the value found in (3.28).

The other bifurcation is the equivalent of Hopf bifurcation and occurs at $\bar{M}(0) = 0$, which gives $\mu_1 = 0$. For the values $\mu_1 \neq 0$, and $\mu_2^2/\mu_1 \neq -16/(7k^2)$, the zeros are simple.

We must give the bifurcation diagram in a full neighborhood of the origin inside the plane $\epsilon_1 = 0$. As in Theorem 4.1, we build this neighborhood as a union of two conic neighborhoods around the ϵ_2 - and ϵ_3 -axes. For the cone around the ϵ_2 -axis we scale $\mu_1 = \pm 1$. Outside the double-zero curve the behaviour is structurally stable. Therefore, for μ_2 in an arbitrary compact space, the behaviour remains the same for μ_0 sufficiently small. This gives a conic

neighborhood of the ϵ_2 -axis. The double-zero curve yields a double limit cycle as in Theorem 3.7.

To obtain a small conic neighborhood of the ϵ_3 -axis we take $\mu_1 = 0$, and scale $\mu_2 = \pm 2$. Then

$$\bar{M}(h) = -4h/7 + (\mu_2 - 8/7)P.$$

$\bar{M}(h) = 0$ is a line through the origin with positive slope if $\mu_2 = +2$, and negative slope if $\mu_2 = -2$. Therefore it has a unique (resp. no intersection) with $P(h) = k\sqrt{h}$. Accordingly the system has a unique (resp. no) limit cycle for $\mu_2 = +2$ (resp. $\mu_2 = -2$). For (μ_0, μ_1) sufficiently small we therefore have a unique (resp. no) limit cycle surrounding the bifurcation diagram of the double-zero eigenvalue (Figure 3).

We can show that the double limit cycle surface in ϵ -space is transversal to $\epsilon_1 = 0$. For $\epsilon_1 = 0$, its equation is given by (4.4), i.e.,

$$F = \epsilon_3^2 - 16/(7k^2)\epsilon_2 + o(\epsilon_2) = 0$$

(since $\epsilon_2 = \pm\delta^4$). The universality of the double limit cycle bifurcation gives rise to a function $G(\epsilon_1, \epsilon_2, \epsilon_3)$ such that the system has a double limit cycle precisely when $G = 0$. Since G coincides with F on $\epsilon_1 = 0$ and $\partial F/\partial\epsilon_2 \neq 0$ then $G = 0$ is equivalent to $\epsilon_2 = \epsilon_2(\epsilon_1, \epsilon_3)$.

4.2. Bifurcation diagram of (2.6) in the case $\eta = 1$.

THEOREM 4.3. *The bifurcation diagram of (2.6) for $\eta = 1$ is a cone. The intersection of the bifurcation diagram with a half-sphere in $\epsilon_1 \leq 0$ is given by Figure 12. The bifurcation diagram is the same as for the cusp of order 3.*

Proof. The proof is similar to Theorem 4.1, but much simpler, since all interesting behavior occurs in the half-plane $\epsilon_1 \leq 0$. The bifurcation diagram is the same as in [11], with homoclinic loop replaced by heteroclinic loop. In this case there is no problem to extend the results obtained in a domain in (x, y) -space depending on δ to a fixed domain in (x, y) -space, since the limit cycles must always lie in the region limited by the separatrices of the saddle points. This region is included in the rescaled domain.

5. Application to the 1:2 resonance of codimension 3. Studying bifurcations of symmetric vector fields under a rotation of order q yields information about Hopf bifurcation for a fixed point of a diffeomorphism F in the plane, with eigenvalues $e^{2\pi ip/q}$: to arbitrary high order, the map F^q can be identified with the flow map of a symmetric vector field having a double-zero eigenvalue, ([3], [4], [10], [23], [25]). The fixed point of the diffeomorphism (which cannot disappear during the bifurcation process) is sent to the origin. To each periodic point of order q correspond q equilibrium points of the vector field, while there is a periodic solution for each invariant closed curve. Resonance of order 2 (also

called 1:2 resonance) which is the one considered here, occurs when we have a pair of eigenvalues equal to -1 , with a Jordan block of order 2. The bifurcation diagram of system (2.6) yields information on the bifurcation diagram for:

$$(5.1) \quad F(x, y) = (-x + y, \epsilon_1 x + (\epsilon_2 - 1)y \pm x^3 + \epsilon_3 x^2 y - x^4 y + y o(|x, y|^5)).$$

The interpretation is conventional. Two kinds of bifurcations cause difficulties. The coalescence of two invariant closed curves, which is a very simple process for vector fields, can be a very complex process for diffeomorphisms when the diffeomorphism has a rational rotation number along invariant closed curves ([8] and [9]). The homoclinic bifurcations are also a long and complex process, since the stable and unstable manifolds of fixed points can have transversal intersections (Figure 13). We may therefore conclude that the bifurcation diagram of vector field (2.6) yields large-scale bifurcation diagram for the diffeomorphism.

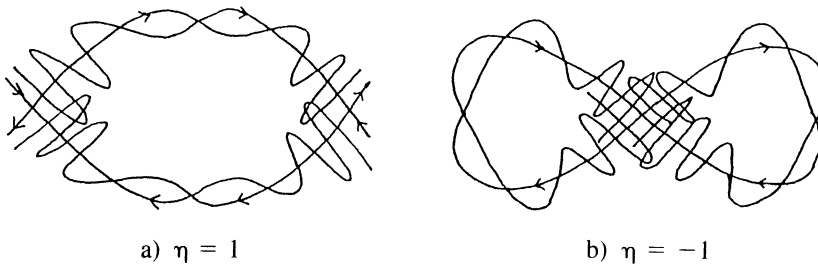


Figure 13. Transversal intersection of stable and unstable manifolds.

Acknowledgements. The authors wish to thank the referee for comments which helped improve the final version of this paper.

REFERENCES

1. A. A. Andronov, E. A. Leontovich, I. I. Gordon and A. G. Meier, *Theory of bifurcations of dynamical systems in the plane*, Israel program of scientific translations, Jerusalem (1971).
2. V. I. Arnold, *Lectures on bifurcations and versal families*, Russian Math. Surveys 27 (1972), 53–123.
3. ——— *Loss of stability of self-oscillations close to resonances and versal deformations of equivariant vector fields*, *Funct. Anal. Appl.* 11 (1977), 1–10.
4. ——— *Geometric methods in the theory of ordinary differential equations* (Springer-Verlag, New York, Heidelberg, Berlin, 1982), (Russian original, 1977).
5. R. I. Bogdanov, *Bifurcation of a limit cycle for a family of vector fields on the plane*, *Trudy Seminar Petrovskii* (1976), (in Russian), *Sel. Math. Sov. I* (1981) (in English), 373–387.
6. ——— *Versal deformation of a singular point of a vector field on the plane in the case of zero eigenvalues*, *Trudy Seminar Petrovskii* (1976), (in Russian), *Sel. Math. Sov. I* (1981) (in English), 388–421.
7. J. Carr, *Applications of center manifolds* (Springer-Verlag, New York, Heidelberg, Berlin, 1981).

8. A. Chenciner, *Bifurcation de points fixes elliptiques. I Courbes invariantes*, Publ. Math. IHES 65 (1985), 67–127.
9. ——— *Bifurcation de points fixes elliptiques. II Orbites périodiques et ensembles de Cantor invariants*, Inventiones Math. 80 (1985), 81–106.
10. S. N. Chow, C. Li and D. Wang, *Center manifolds, normal forms and bifurcations of vector fields*, book, in preparation.
11. F. Dumortier, R. Roussarie and J. Sotomayor, *Generic 3-parameter families of vector fields on the plane, unfolding a singularity with nilpotent linear part. The cusp case of codimension 3*, Ergodic Theory Dynamical Systems 7 (1987), 375–413.
12. ——— *Generic 3-parameter families of planar vector fields on the plane, unfoldings of saddle, focus and elliptic singularities with nilpotent linear parts*, preprint (1988).
13. J. Guckenheimer, and P. Holmes, *Nonlinear oscillations, dynamical systems and bifurcations of vector fields* (Springer-Verlag, New York, Heidelberg, Berlin, 1983).
14. E. I. Horozov, *Versal deformations of equivariant vector fields under symmetries of order 2 and 3*, Trudy Seminar Petrovskii 5 (1979), 163–192.
15. P. Joyal, *The cusp of order n*, to appear in J. Differential Equations.
16. M. G. Lassalle, *Une démonstration du théorème de division pour les fonctions différentiables*, Topology 12 (1973), 41–62.
17. Li Chengzhi and C. Rousseau, *A system with three limit cycles appearing in a Hopf bifurcation and dying in a homoclinic bifurcation. The cusp of order 4*, J. of Differential Equations 79 (1989), 132–167.
18. P. Mardesic, *The number of limit cycles of polynomial deformations of a Hamiltonian vector field*, preprint (1988).
19. G. S. Petrov, *Elliptic integrals and their nonoscillation*, Funct. Anal. Appl. 20 (1986), 37–40.
20. V. Poenaru, *Analyse différentielle*, Springer Lecture Notes 371 (Springer-Verlag, New York, Heidelberg, Berlin, 1974).
21. R. Roussarie, *On the number of limit cycles which appear by perturbation of separatrix loop of planar vector fields*, Bol. Soc. Bras. Mat. 17 (1986), 67–101.
22. ——— *Déformations génériques des cusps*, Astérisque 150–151 (1987), 151–184.
23. C. Rousseau, *Codimension 1 and 2 bifurcations of fixed points of diffeomorphisms and of periodic orbits of vector fields*, to appear in Annales Mathématiques du Québec.
24. Shi Songling, *A method of constructing cycles without contact around a weak focus*, J. of Differential Equations 41 (1981), 301–312.
25. F. Takens, *Forced oscillations and bifurcations*, in *Applications of global analysis I*, Comm. Math. Inst. Rijksuniversiteit Utrecht (1974), 1–59.
26. F. Takens, *Singularities of vector fields*, Publ. Math. I.H.E.S. 43 (1974), 47–100.

*Peking University,
Beijing, People's Republic of China;
Université de Montréal,
Montréal, Québec*